

Thermography improvements using ultraviolet pyrometry.

by P. HERVE¹ and A. MOREL²

¹ Laboratoire d'Energétique et d'Economies d'Energie, Université Paris X, 1 chemin Desvallières, 92410 Ville-d'Avray, France ; ² LASUR, 119Bis rue de Colombes, 92600 Asnières, France.

Abstract

Thermography in the UV range allows to nearly get rid of the effects of emissivity, which is the main difficulty of quantitative IR thermography. In the UV range, the strong increase of luminance as a function of temperature - it doubles every 20°C around 700°C - hides the effects of emissivity and allows for an exceptional sensitivity from 600°C on. Another important advantage of UV is due to the fact that natural and artificial radiating sources disturb the measurement ten times less than in the IR. Examples of applications to melting phenomena, temperature rises under shock and simultaneous temperature and emissivity cartography are presented.

1. Introduction

Thermography, the only technique which at present allows to obtain the superficial temperature of an object without contact and disturbance, is still considered by users as an essentially qualitative method. Indeed, available apparatus give luminance maps which are often to excess called temperature maps. Actually, luminance depends on temperature according to Planck's law ; but it is at the same time proportional to emissivity, a factor which ranges from 0 to 1 and which is strongly dependant on the material investigated, its surface state and the aiming angle. In all quantitative operations, we thus try to obtain the temperature of a surface or cloud of particles from a single measurement depending simultaneously on temperature, emissivity and room radiations reflected by the aimed material. This difficulty, due to the imbrication of parameters, is not solved in the usual thermographic systems which design looks for maximum detectivity. Most manufacturers have chosen to use the windows of atmospheric transparency located close to the maximum of Planck's curve, that is 3-5µm or 8-12µm. The images realised in these wavelength fields are quite spectacular but do not allow to dissociate temperature and emissivity effects, particularly so in the case of metallic surfaces. Shorter wavelength, in the VIS or near IR, do not seem to have attracted the attention of system designers ; maybe so because it is impossible to work with such wavelengths in the presence of natural or artificial lighting.

In the procedure presented here, we go back to the basic physical phenomena involved in the emission of thermal radiations. The separation between temperature and emissivity effects is then obtained by choosing the shortest wavelength to be compatible with a sufficient photonic emission. Beyond the VIS range, in which measurements can only be carried out in the utmost darkness, we reach the UV domain in which natural radiating sources are strongly absorbed or diffused by ozone atmospheric layer and plain glass windows and where artificial lighting sources are limited due to safety regulations. Therefore, it is in the UV domain that we have developed the quantitative thermographic applications presented below [1,2].

2. Influence of the working wavelength over the sensitivity

Radiation sensors are sensitive to luminance L , which is expressed by Planck's law :

$$L_{\text{measured}}(\lambda, T) = \varepsilon_{\lambda, T, \theta} \cdot A \cdot \frac{1}{e^{\frac{c_2}{\lambda T}} - 1} \quad (1)$$

where :

T stands for the temperature in Kelvin ;
 λ wavelength in μm ;
 $\epsilon_{\lambda, T, \theta}$ material emissivity ;
 A is an apparatus constant ;
 $C_2 = 14400 \mu\text{m.K}$.
 If $\lambda \cdot T < 3000 \mu\text{m.K}$, this formula can be simplified using Wien's approximation :

$$L_{\text{measured}}(\lambda, T) = \epsilon_{\lambda, T, \theta} \cdot A \cdot e^{-\frac{C_2}{\lambda T}} \quad (2)$$

The thermometric effect, that is the sensitivity of the measurement, is then obtained by differentiating (2) :

$$\frac{dL}{L} = \frac{d\epsilon}{\epsilon} - \frac{C_2}{\lambda T} \cdot \frac{dT}{T} \quad (3)$$

The measurement sensitivity varies as the inverse of wavelength. *Figure 1* represents the sensitivity as a function of T and λ . Arbitrarily, we have considered that a sensitivity below 0,1% per °C wouldn't allow to distinguish between the temperature and emissivity effects. In the UV range, sensitivity is about 10 times greater than in the IR. For example, at 700°C, the luminance measured at $\lambda=0,4\mu\text{m}$ doubles every 20°C. Actually, it is the random character of photon emission process which constitutes the equivalent of the N.E.P. of detectors used in usual systems. We can then determine a minimum detectable temperature difference such that :

$$\Delta T = \text{Cte} \cdot T^2 \cdot e^{\frac{C_2}{\lambda T}} \quad (4)$$

For instance, if the noise sources limit the detectivity value to 0,1°C at 727°C, it will be 0,05°C at 827°C and 0,005°C at 927°C. At high temperatures, sensitivity is only limited by sensor dynamics and, for CCD cameras, by the reading noise.

3. Environment radiation effects as a function of the working wavelength.

The detector receives the radiations emitted by the aimed object added to the radiations emitted by the surrounding heat sources and reflected by the object surface. One can then write :

$$L_{T_{\text{measured}}} = \epsilon L^{\circ}_{\lambda, T} + \rho \epsilon_s L^{\circ}_{\lambda, T_s} \quad (5)$$

Where ϵ_s and T_s stand for emissivity and temperature of the surrounding sources ;
 $\rho = 1 - \epsilon$, is the reflection coefficient of the aimed material.

Measured temperature in these conditions can be obtained from :

$$L_{T_{\text{measured}}} = \epsilon L^{\circ}_{\lambda, T_{\text{measured}}} \quad (6)$$

supposing that the material emissivity is known. This measured temperature is always higher than the real temperature.

Figure 2 represents the error variation as a function of the wavelength presuming $\epsilon = \text{cte}$. The UV range measurement is obviously much better than the IR one and this advantage is still greater for metals as ϵ increases when λ decreases.

Going back to equation (5), the reflection term can be rewritten as :

$$L^{\circ}_{\lambda, T_{\text{measured}}} = L^{\circ}_{\lambda, T} + (1 - \epsilon) \epsilon_s / \epsilon L^{\circ}_{\lambda, T_s} \quad (7)$$

The error is very high with IR and a IR camera user has better to display an emissivity overvalued and close to 1. We can then understand why many emissivity values one can find in handbooks are too high, because authors didn't always take care of the surrounding radiations.

4. Emissivity effects as a function of the working wavelength.

Suppose that the emissivity of the material we look at is independent of wavelength and that the Wien's approximation of Planck's law can be used. Then :

$$\frac{1}{T_1} = \frac{1}{T} - \frac{\lambda}{C_2} \cdot \text{Ln}\epsilon \quad (8)$$

The error due to the emissivity is proportional to the value of the wavelength. Passing from IR to UV range, we divide wavelength by ten, so the error. This effect shows another way to explain the sensitivity increase in the UV range. As an example, let's suppose $\epsilon = 0,4$ and $T = 740^\circ\text{C}$. Let's then take different values of the estimated emissivity. *Figure 3* shows that an emissivity variation of +50% gives a $\pm 15^\circ\text{C}$ error on the measured value of T in the UV range and absurd values in the IR range either at $5\mu\text{m}$ or at $10\mu\text{m}$. As we already mentioned it, this effect is still stronger in the case of metals for which emissivity increases as wavelength decreases.

5. Simultaneous measurements of temperature and emissivity

Emissivity has usually been considered as a perturbation factor in the measurement of the true temperature. In many industrial cases, what is really looked for is the knowledge of the physico-chemical state of the material. Then the temperature is only needed as an indication. Emissivity however relates directly to the state of the material. First order phase changes are characterised by a discontinuity in the emissivity. Second order phase changes show an inflexion point of the emissivity vs. temperature curve. But to obtain the emissivity value we firstly need to measure the surface temperature. We then realised a thermographic system where true temperature is measured in the UV range (intensified camera centred on $\lambda = 0,37\mu\text{m}$). Another measurement in the IR ($\lambda = 5\mu\text{m}$) allows to get the emissivity at the said wavelength. *Figure 4* shows a scheme of the apparatus and the temperature and emissivity curves obtained for one pixel in cooling a melted Nickel sample. True temperature in the UV range is obtained with a few degrees error assuming that the UV emissivity of Nickel equals 0,5. The curve shows a slow decrease of the temperature until a value below the solidification temperature, then a sharp increase, and finally a very quick decrease. Looking at the emissivity evolution, one can see the phase change. During the melted then the overmelted phases, the emissivity remains equal to 0,25. At the solidification point, emissivity drops instantly to 0,20. UV range image shows heat waves which correspond to convection currents in the melted metal.

6. Applications examples

We show several examples where UV thermography allows to minimise some problems met in the IR range. A first apparently simple case, displayed on *figure 5*, shows the temperature map on an aluminium plate on which a grid pattern was painted using VELVET 3M black painting. One can see on the IR image that the apparent temperature varies from 592°C to 405°C when the true plate temperature remains close to 600°C . In the UV range, the difference between the aluminium and the painted part apparent temperatures is divided by ten (20°C). The image is less spectacular but ten times more accurate than in the IR range. On *figure 6* we show an example of UV thermography on a silicon bath which was induction heated in a cold crucible. The measurement time is $1\mu\text{s}$. We can see the solidification dendrites. The melted zones look colder as emissivity of the liquid is smaller than that of the solid. *Figure 6* displays a zoom on the same image after computer processing taking into account the emissivity. One can see a columnwise solidification process.

Another application is shown concerning a jet of particles. The final purpose was to get a knowledge of the temperature repartition in the jet of a solid propergols propeller. Two measurement wavelengths at $0,36\mu\text{m}$ and $0,39\mu\text{m}$ were simultaneously analysed using two photomultipliers tubes and scanning mirrors. The system was mounted 7 meters close to a large size propeller, worked outside at noon in August, and resisted to 180 dB acoustic

vibrations. An image is displayed on *figure 7*. A 10^9 variation range of luminance values allowed to obtain a temperature cartography between 1000°C-2500°C.

Finally, we show on *figure 8* thermomechanical effects on shear bands obtained with a Titanium TaV6 sample. It is the first time, as far as we know, that such a thermography was obtained. Adiabatic shear bands are very transitory phenomena lasting less than 50µs [4]. and covering microscopic areas (10x500µm). In order to increase the measurement sensitivity, we used an interferential filter centred in the red. A simultaneous measurement with an InSb detector showed a $\alpha \leftrightarrow \gamma$ phase change at 950°C and allowed for the calibration of the experiment. The measured temperatures [5], which exceed 1400°C, are greater than the corresponding data that can be found for Titanium in the literature. These results suggest to reconsider classical interpretation of that kind of ruptures.

7. Conclusion and perspectives

Thermography in the UV range enables research laboratories and industrial users to obtain, by means of a photon counting technique, true surface temperatures above 500°C. For example, with the equipments available right now, UV thermography allows to determine the true temperature distribution of a steel sample, whatever its physico-chemical state, with a $\pm 5^\circ\text{C}$ accuracy around 750°C which is an usual value for annealing.

A complementary measurement in the IR range gives an emissivity cartography which allows to characterise the first order (liquid-solid) and second order (for instance $\alpha \leftrightarrow \gamma$) phase changes or, more simply, the apparition of an oxidisation. A fruitful application will be the control of industrial equipments from variations in the emissivity of the processed body [6]; for example heat treatment after cold lamination of steel sheets.

UV bicolour thermography can also be used to analyse the temperature distribution in incandescent particles jets originating from combustion such as solid propergols. The accuracy is then of the order of 30°C around 2500°C.

In the case of industrial applications, materials are often heated up in an oven that is in a still hotter environment. In that cases, IR thermography determines an intermediate value between the target surface temperature and the environment temperature. Working in the UV range allows to reduce by a 10 factor the measurement error without any dazzling due to VIS light sources.

The improvements we are presently involved in deal with a decrease in the minimum observable temperature and a reduction in the minimum measurement time.

The first point is essentially related to the noise of the detector matrix and can be improved by image processing.

Some applications, such as thermal effects observation consecutively to a shock, need an exposure time close to 1 microsecond. Unsteady states can then be studied.

REFERENCES

- [1] HERVÉ (P.). - *Pyromètre à ultraviolet*. Patent F880387, March 1988.
- [2] HERVÉ (P.), MASCLÉ (P.) and LEFEVRE (A.). - *Ultraviolet pyrometry*. TEMPMEKO 90, Helsinki, Sept. 1990.
- [3] TOULOUKIAN and DE WITT. - *Thermal Radiative properties*, Plenum, New York, 1970.
- [4] MARCHAND (A.) and DUFFY (J.). - *An experimental study of the formation process of adiabatic shear bands in a natural steel*. J. of Mech. and Phys. of solids., Vol. 36, N°3, pp. 251-283, 1988
- [5] PINA (V.) and HERVÉ (P.). - *Temperature history of adiabatic shear bands in metals*, 14th International CODATA '94 Conference, Chambéry, 18-22 Sept. 1994.
- [6] MEUNIER (M.), HERVÉ (P.) et al. - *Measurement of a steel sheet temperature during continuous annealing by UV Pyrometry*, 6th International Congress for sensors and microsystems technology, Nuremberg, Oct. 11-14 1993.

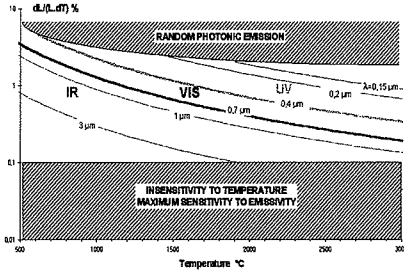


Figure 1. Sensivity vs wavelength.

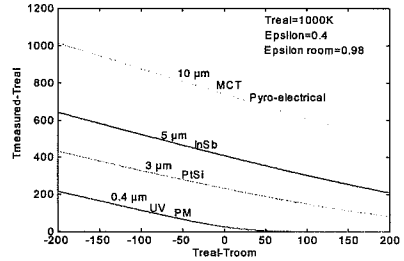


Figure 2. Environment perturbation vs wavelength.

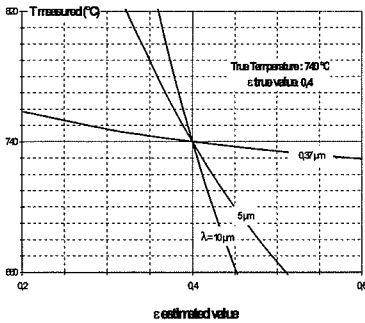


Fig. 3. Error induced by ϵ vs λ .

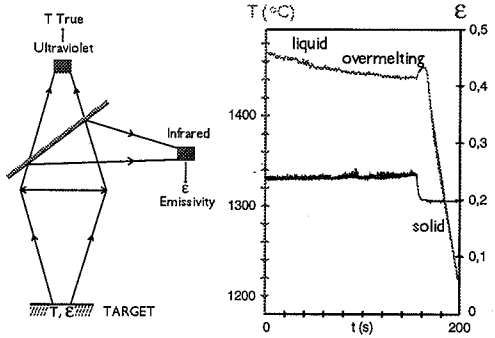
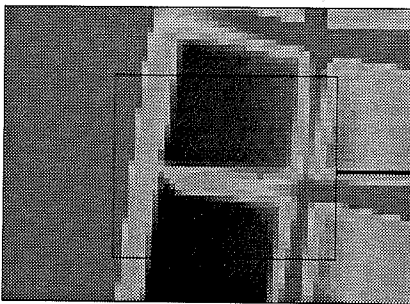
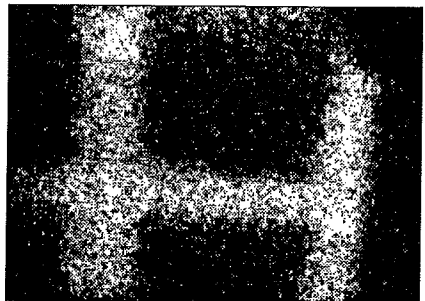


Fig. 4. Simultaneous measurement of T and ϵ . Example of Nickel solidification.



T paint = T aluminium = 600°C
 T_{paint} = 592 °C
 T_{aluminium} 405°C
 $\lambda = 3 \mu\text{m}$



T paint = T aluminium = 600°C
 T_{paint} = 598°C
 T_{aluminium} 578°C
 $\lambda = 0,37 \mu\text{m}$

Figure 5. Simultaneous view of aluminium and paints in IR and UV.

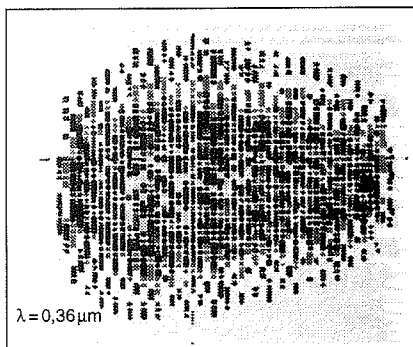
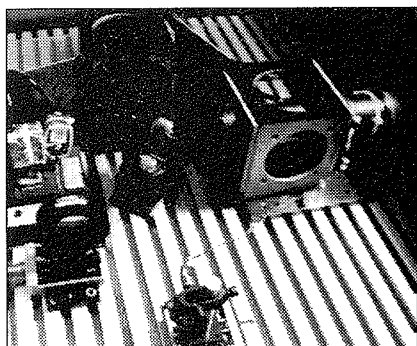


Figure 6. Bi-color UV camera and jet of particles thermography.

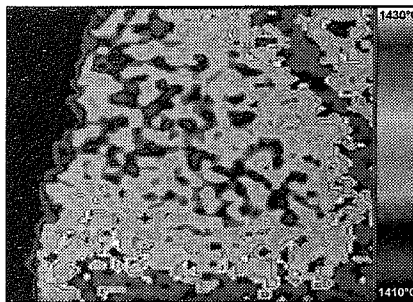
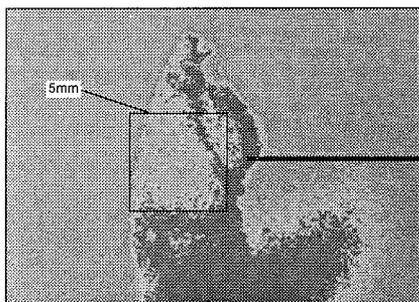


Figure 7. Silicon fused : dendrites and columnwise solidification process (measurement time = 1 μs).

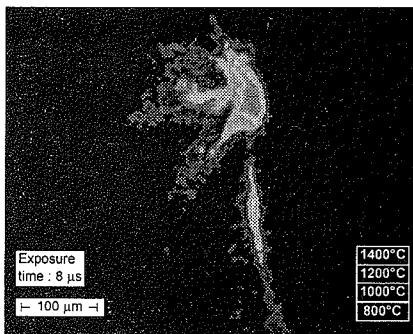
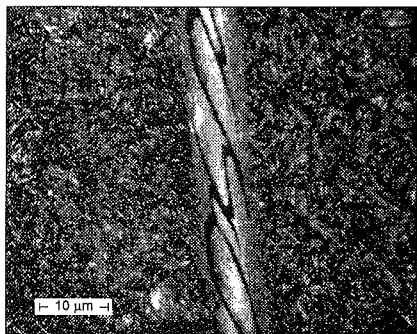


Figure 8. Adiabatic shear band. Micrography (steel) and thermography (Ta6V).